

Effective Load Carrying Capacity of Solar PV Plants: A case
study across USA

A Thesis

Presented in Partial Fulfillment of the Requirements for the Degree
Master of Science in the Graduate School of The Ohio State
University

By

Dhruv Gami,

Graduate Program in Department of Industrial & Systems Engineering

The Ohio State University

2016

Master's Examination Committee:

Dr. Ramteen Sioshansi, Advisor

Dr. Antonio Conejo

© Copyright by

Dhruv Gami

2016

Abstract

Abstract:

Evaluating the capacity value of solar PV plants can pose significant challenges due to their dependence on geographic and climatic conditions, which are highly variable and uncertain. Also, the way the data are recorded gives a significant variation in capacity value estimates. In this dissertation, different capacity value metrics are reviewed, several case studies are summarized and capacity value using the Effective Load Carrying Capability (ELCC) metric is estimated for 100 MW PV plants located across North America. ELCC estimates using hourly and minute-based solar data are compared, ELCCs are computed after shifting the load data ahead and behind by one hour to account for the sloppiness in reporting load data, and ELCC estimates using modeled and measured solar data are compared.

Acknowledgments

I would like to express my sincere gratitude to my advisor, Dr. Ramteen Sioshansi for his patience, motivation, and continuous support throughout my graduate school studies. His guidance helped me throughout the research work. I'm grateful for his mentorship and look forward to keeping in touch in the future.

I would like to thank NREL for supporting part of my graduate studies at The Ohio State University and for giving me an opportunity to work on this project. This work was supported by the U.S. Department of Energy (DE-AC36-08GO28308) and by the Alliance for Sustainable Energy, LLC (AGN-2-22165-01). Also, I would like to thank everyone at NREL, especially Paul and Andrew who helped me throughout the research work.

I would like to thank all my previous bosses from Jyoti Structures Ltd., who were also my mentors, and who worked on my transition from a college graduate to a professional.

I would thank my roommates, and my friends from Sankalpa, who have been there for me like a family. I would also like to thank all my friends back home.

Finally, I'd like to thank my parents, brother, and grandmother. Without their support this would not have been possible.

Also, I'd like to thank my late grandfather who has been an inspiration throughout my life.

Vita

Jul, 2011 B.S. Mechanical Engineering

Aug, 2011 - July, 2013 Executive Engineer,
Jyoti Structures Ltd, Mumbai, India.

Jan, 2014-present M.S. Student,
Department of Integrated Systems En-
gineering,
The Ohio State University.

Fields of Study

Major Field: Industrial and Systems Engineering

Specialization: Operations Research

Table of Contents

	Page
Abstract	ii
Acknowledgments	iii
Vita	iv
List of Tables	vii
List of Figures	viii
1. Introduction	1
2. Literature Survey	4
2.1 Reliability-Based Methods	5
2.1.1 Effective Load Carrying Capability (ELCC)	7
2.1.2 Equivalent Conventional Power (ECP)	8
2.1.3 Equivalent Firm Capacity (EFC)	9
2.2 Approximation Methods	9
2.2.1 Capacity Factor Based Approximations	10
2.2.2 Garver approximation based methods:	11
2.2.3 Z-Method:	13
2.3 Other Methods	14
3. Case Studies	19

4.	Data and Model	23
4.1	Photovoltaic Data and Model	23
4.2	Conventional Generators	24
4.3	Load Data	25
4.4	Example: Compute ELCC of 35 MW Solar PV plant	26
5.	Results: Case Study across North America - Solar PV	30
5.1	Comparison of ELCCs computed using hourly and subhourly solar data	34
5.2	Comparison of ELCC computed using original load data and ELCC computed after load data is shifted one hour ahead and behind	41
5.3	Comparison of ELCC computed using measured (surfrad) data and ELCC computed using modeled (nsrdb) data	49
6.	Conclusion and Future Work	56
	Bibliography	57

List of Tables

Table	Page
4.1 Location information	24
4.2 Utility load data (GW)	26
4.3 Example: conventional generators available	26
4.4 Example: Capacity Outage Probability Table (COPT)	27
4.5 Example: LOLE computed for the base case	28
4.6 Example: ELCC computed for 35 MW solar PV plant	29
5.1 Average Hourly and Subhourly ELCCs and Absolute Value of Differences in ELCCs Estimated Using Hourly and Subhourly Solar Data	31
5.2 Average Differences in ELCCs Estimated Using Load Shifted One Hour Backward and Forward One Hour and Original Load Data	32
5.3 Average, Maximum and Minimum Difference in ELCC Estimates using Measured and Modeled Solar Radiation Data.	32

List of Figures

Figure	Page
2.1 Illustration of LDC method.	15
2.2 Illustration of the Demand-Time Interval Matching (DTIM) method.	16
2.3 Illustration of SLC method.	17
5.1 Nevada(2006) - Average load, average hourly PV output and average minute based PV output for hours of the day for all the days of the year.	35
5.2 Nevada(2006) - Load, hourly PV output and subhourly PV output on the highest load day.	36
5.3 Montana(2005) - Average load, average hourly PV output and average minute based PV output for hours of the day for all the days of the year.	37
5.4 Montana(2005) - Load, hourly PV output and subhourly PV output on the highest load day.	38
5.5 Nevada(2007) - Average load, average hourly PV output and average minute based PV output for hours of the day for all the days of the year.	39
5.6 Nevada(2007) - Load, hourly PV output and subhourly PV output on the highest load day.	40
5.7 Nevada(2011) - Average load, average load shifted 1 hour back, average load shifted 1 hour ahead and average hourly PV output for hours of the day for all the days of the year.	43
5.8 Nevada(2011) - Load, load shifted 1 hour back, load shifted 1 hour ahead and hourly PV output on the highest load day.	44

5.9	Mississippi(2003) - Average load, average load shifted 1 hour back, average load shifted 1 hour ahead and average hourly PV output for hours of the day for all the days of the year.	45
5.10	Mississippi(2003) - Load, load shifted 1 hour back, load shifted 1 hour ahead and hourly PV output on the highest load day.	46
5.11	Pennsylvania(2009) - Average load, average load shifted 1 hour back, average load shifted 1 hour ahead and average hourly PV output for hours of the day for all the days of the year.	47
5.12	Pennsylvania(2009) - Load, load shifted 1 hour back, load shifted 1 hour ahead and hourly PV output on the highest load day.	48
5.13	Nevada(2012) - Average load, average PV output from measured and modeled radiation data for hours of the day for all the days of the year.	50
5.14	Nevada(2012) - Load and PV output on the highest load day.	51
5.15	Mississippi(2013) - Average load, average PV output from measured and modeled radiation data for hours of the day for all the days of the year.	52
5.16	Mississippi(2013) - Load and PV output on the highest load day.	53
5.17	Colorado(2009) - Average load, average PV output from measured and modeled radiation data for hours of the day for all the days of the year.	54
5.18	Colorado(2009) - Load and PV output on the highest load day.	55

Chapter 1: Introduction

Electricity is a commodity in which supply must be balanced with demand instantaneously at all times. The system delivers energy to its consumers but if at any time there is insufficient generating capacity to meet demand, then the demand must be reduced to ensure system stability. Thus electric generation facilities provide value by supplying energy, but they also deliver value through their capacity contribution. Capacity value (or capacity credit) measures the contribution of a facility or a group of facilities to the reliability of the overall electrical supply system. This is usually assessed with respect to system adequacy (whether there is sufficient capacity available to meet the demand at all times), rather than system security (the ability of the system to withstand sudden faults or disturbances) [3, 13, 22, 6].

Over the past decade, the United States and other countries are restructuring their power sectors and framing policies to utilize generating resources to reliably meet electricity demand. This is a major problem faced by power system planners. Generator outages can occur due to mechanical failures, planned maintenance, or lack of generating resource. Such failures may leave a power system with insufficient generating capacity to meet demand. Though there are a variety of generation technologies to choose from, there has been an increasing interest in the use of renewables.

The issue faced in capacity planning with renewable is because of the variable and uncertain nature of their real-time output. Thus, accurate estimates of capacity value of such resources are vital [3, 13, 22, 6].

Previous analyses estimate the capacity value of wind, photovoltaics, and concentrating solar power (CSP) resources. They show that these resources have non-zero capacity values that can range from 5% - 95% of maximum generating capacity. This range reflects the effect of technology, geography, demand patterns, and the coincidence between real-time generation and demand. It also reflects the decreasing capacity value of additional renewable generators [13, 19, 11, 14, 18]. All these analyses use a mix of reliability-based and statistical approximation techniques. These techniques estimate the probability that a power system experiences an outage event, which is an event when the available generating capacity is less than the demand. The capacity value is determined based on the contribution of a generator towards reducing this probability [14].

In this study, we estimate the capacity value of solar PV plants using the capacity value estimation metric - effective load carrying capability (ELCC). The ELCC of 100 MW PV plant varies from 5 MW to 42 MW based on the location. We compare the ELCCs computed using hourly solar data and subhourly solar data for PV plants, and we find that the absolute difference can go upto 16% (Table: 5.1) for a PV plant located in Montana in the year 2005. This shows that using hourly solar data can introduce significant errors in estimating ELCCs for a particular year. Though, this error smooths out when we use multiple years of data to estimate the ELCCs.

We also compare the ELCCs computed using the original load data with ELCCs computed using load data shifted one hour ahead and one hour behind. This is to see if ELCCs are sensitive to the sloppiness in the reported load data. We find that the ELCCs are highly sensitive to these load shifts for solar PV plants. ELCCs for solar PV plants, computed using original load data differ in the range of -37% to +42% from ELCCS computed using the shifted load data (Table: 5.2). The large error is persistent throughout the years studied for each location and it does not smooth out.

This thesis also compares ELCCs computed using measured and modeled solar data. We have access to satellite data which is the modeled data for locations on a $4km^2$ grid across North America. It is difficult and expensive to get real-time measured data for these many locations. Thus, we want to see if modeled data does justice in estimating the ELCCs. From the results, we find that the maximum error in certain cases such as PV located in Mississippi and Pennsylvania can go up to 104% and 71% respectively (Table: 5.3) which shows that ELCC estimates using modeled solar radiation data may not give accurate results.

The rest of this thesis is organized as follows:

In Chapter 2, we review the different capacity value techniques being used today. Chapter 3 summarizes the different case studies on capacity value estimation for Solar Photovoltaic and discusses the results. Chapter 4 presents case study on ELCC estimates for Solar PV plants across North America and outlines the data and model used to estimate the ELCCs. Chapter 5 gives the results of this case study on ELCC estimates of PV plants. Chapter 6 concludes this thesis.

Chapter 2: Literature Survey

This chapter reviews different capacity value estimation techniques, which are being used today, and summarizes different case studies on capacity value estimation for solar and wind power.

To discuss the different capacity value estimation techniques, we define the following nomenclature as follows:

T	Time index set
T'	subset of hours used in capacity factor-based approximation
p_t	Loss of Load Probability
L_t	Hour- t load
G_t	Generation capacity at time t
ϵ	Loss of Load Expectation (LOLE) of base system without PV
ϵ^{ELCC}	LOLE with PV in effective load carrying capability (ELCC) calculation
ϵ^{PV}	LOLE with PV in equivalent conventional power (ECP) calculation
ϵ^B	LOLE with benchmark unit added in ECP calculation
V_t	Generating capacity available from PV plant in hour- t
\bar{L}	Constant loaded added in each hour in ELCC calculation

B_t	Generating capacity available from benchmark unit in hour t in ECP calculation
w_t	Hour- t weight used in capacity factor-based approximation
\bar{V}	Rated capacity of PV plant
\bar{G}	Nameplate conventional generating capacity
m	System characteristic
π_ω	Probability PV plant is in state ω
V_ω	PV capacity unavailable in state ω
Z	Z statistic
Ω	Index set for PV plant states in multi-state ELCC approximation
S_t	Hour- t surplus generation capacity
μ_S	Mean of S_t
μ_{PV}	Mean hourly generating capacity available from PV plant
σ_S	Standard deviation of S_t
σ_{PV}	Standard deviation of hourly generating capacity available from PV plant

2.1 Reliability-Based Methods

There are a number of techniques which are used to evaluate the capacity value of conventional as well as renewable generators. Reliability-based methods are among the most robust and widely accepted of all of these because they fully account for the effect of a generator on the reliability of a power system [13, 11, 14, 18, 7, 15, 17]. These techniques are based on a standard reliability metric - the loss of load

probability (LOLP). Loss of load occurs when the system load exceeds the generating capacity available for use. Thus, LOLP is defined as the probability that generator or transmission outages leave the system with insufficient capacity to serve the load in a given period of time.

$$p_t = Prob(G_t < L_t) \quad (2.1)$$

Another reliability index, loss of load expectation (LOLE) is usually used with the LOLP. It is defined as the sum of LOLPs over a planned time period and it gives the expected number of outage periods within that time period. The LOLP is given by:

$$\epsilon = \sum_{t \in T} p_t \quad (2.2)$$

Other reliability metrics, such as loss of energy probability, loss of energy expectation, loss of load frequency, and loss of load duration can also be used. These metrics are less common. In estimating the capacity value of renewables, LOLE-based methods are widely used. LOLPs are usually modeled on hourly time steps and LOLEs are computed over a year. Conventional generator and transmission outages are modeled using equivalent forced outage rate (EFORs) which capture the probability of a failure at any given time. Reliability based methods include the effective load carrying capability (ELCC), equivalent conventional power (ECP) and equivalent firm power (EFP).

2.1.1 Effective Load Carrying Capability (ELCC)

The ELCC of a generator is defined as the amount by which the system's loads can increase, when the generator is added to the system while maintaining the same reliability index (as measured by LOLE). The ELCC of PV is calculated by first calculating the total loss of load probability (LOLP) given by equation 2.1 of the original system without the PV. This is typically done keeping the time period of one year. This probability function accounts for generator and other failures. Generator failures are often modeled using an equivalent forced outage rate (EFOR). The LOLE is then calculated, which is given by equation 2.2 above. The system is then modified to give a standard LOLE of 1 day in 10 years. This does not give a true measure of the adequacy of the system because the true LOLE is different. However, it allows for PV's contribution to be assessed and compared against other system that use this standard value. Next, the PV plant is added to generator mix and a fixed load, \bar{L} , is added to each hour, giving a new LOLE:

$$\epsilon^{ELCC} = \sum_{t \in T} Prob(G_t + V_t < L_t + \bar{L}) \quad (2.3)$$

where the probability function also accounts for the probability of real-time solar availability. The fixed load added to each hour is iteratively adjusted until the LOLE of the system with the PV and added loads is the same as that of the base system i.e.

$$\epsilon = \epsilon^{ELCC} \quad (2.4)$$

The PV plant's ELCC is defined as the value of \bar{L} that achieves condition 2.4.

2.1.2 Equivalent Conventional Power (ECP)

The ECP of a generator, g , is defined to be the capacity of a benchmark unit, which is assumed to have a positive EFOR, that can replace g while maintaining the same LOLE. In this method, the renewable generator's capacity value can be benchmarked against a conventional resource. For example a 100 MW PV plant may have a capacity value equivalent to a 30 MW natural gas fired combustion turbine. The ECP of a PV generator is calculated by first computing the LOLE of the system when the PV is added as:

$$\epsilon^{PV} = \sum_{t \in T} Prob(G_t + V_t < L_t) \quad (2.5)$$

The LOLE of the system when only the benchmark plant (i.e. without the PV) is added is also computed as:

$$\epsilon^B = \sum_{t \in T} Prob(G_t + B_t < L_t) \quad (2.6)$$

Here the probability function takes into consideration the likelihood of the conventional generator (benchmark unit) failing by using its EFOR. The nameplate capacity of the benchmark unit is iteratively adjusted until the LOLE of the system with the benchmark unit is the same as that with the PV plant, or until

$$\epsilon^{PV} = \epsilon^B \quad (2.7)$$

The PV plant's ECP is defined as the nameplate capacity of the benchmark unit that achieves equality 2.7 [13, 14, 2].

2.1.3 Equivalent Firm Capacity (EFC)

The EFC of a generator, g , is defined to be the capacity of a fully reliable generator (i.e., with an EFOR of 0%) that can replace g while maintaining the same LOLE. A generator's ELCC and EFC may differ, because changing the generation mix changes the distribution of the available capacity in a given hour whereas adjusting the loads will not. ECP is similar to EFC except that the generator against which g is benchmarked is not fully reliable, which means it has a positive EFOR [23, 13, 14].

2.2 Approximation Methods

Reliability-based methods are widely accepted and considered to be robust and accurate in giving capacity value estimations. However, they require expensive iterative LOLP calculations, which can be time consuming. Due to seasonal and annual weather patterns, several years' data are required to accurately estimate long-run capacity values of renewables.

Because of these challenges of using reliability-based techniques, approximation techniques are often used to estimate capacity values. Among the approximation methods are capacity-factor based methods [16], Garver's ELCC approximation [7], and the Z method [5]. These methods reduce the computational effort by either approximating the relationship between capacity added and the LOLPs or by focusing on some subset of hours, which are considered to be high risk when the system is likely to experience loss of load. There have been several studies to examine the accuracy of these approximation techniques in estimating the capacity values of wind, CSP, and PV. Milligan and Parsons [16] use three different techniques to estimate the

capacity value of wind. Their first method calculates the capacity factor as the ratio of average output to the total output for the hours during the utility system peak (top 30% hourly peak loads). The second method uses hours in which the risk of not meeting the load is highest i.e. highest LOLP (of the base system without wind). The third method is the weighted average of capacity value during the highest-load hours of the year, using LOLPs as weights. Madaeni et al. [15, 14, 13] compare the capacity factor-based and reliability-based methods applied to CSP and PV showing that these methods can provide relatively accurate approximations.

2.2.1 Capacity Factor Based Approximations

This method approximates the capacity value of a generator as its average capacity factor over a subset of risky periods [14, 17, 16]. This method approximates the capacity value by first determining a subset of hours, T' , with the highest loads, over which the capacity factor is averaged. The weights used in each hour are then computed as:

$$w_t = \frac{p_t}{\sum_{t \in T'} p_t} \quad (2.8)$$

Where the p_t 's are the LOLPs of the base system, without added PV, and are calculated using equation 2.1. The capacity value of the PV plant is approximated as:

$$\frac{\sum_{t \in T} w_t \cdot V_t}{\bar{V}} \quad (2.9)$$

Aguirre et al. [1] approximate the capacity value of wind using LOLP at time of annual peak demand instead of LOLP for each hour. The definition of ELCC for

peak load calculation remains the same as for a year round calculation, except that LOLP used is at time of annual peak demand [1, 11]. Thus, probability distributions for demand and available wind capacity at time of annual peak load are required (the distribution for conventional generation is derived from the COPT calculation, as in the reliability-based ELCC calculation method). To determine the probability distribution of wind capacity either a histogram of hourly load factors for the entire peaking season or a histogram of load factors from hours where demand is within a certain percentage of that year's peak is used. The former has a disadvantage since many days may not be close to annual peak demand whereas the latter ensures greater relevance to peak demand [11].

This is similar to the Time/Season Window (TSW) method, which calculates capacity credits across predefined hours, months, and/or seasons. It is often referred to as the ERCOT method, named after the practice to assign capacity value to wind generators operating in the ERCOT regional reliability council. It is also used by MAPP [19]. The disadvantages of annual peak calculation and TSW method are that there is no obvious way to capture the effect of different grid penetration levels, loss of load at other times of the year outside the selected peak time window are disregarded, and the peak time window may possibly exclude high-risk load hours. Furthermore, it is difficult to obtain a probability distribution of wind or PV at annual peak, and also for the peak load [19, 11].

2.2.2 Garver approximation based methods:

Garver proposed a simplified graphical based approach to calculate the ELCC of an additional generator [7]. This is one of the most widely used methods of capacity

value calculation. The paper proposes ELCC approximation using the exponential risk function:

$$\epsilon \approx \sum_{t \in T} B \cdot \exp\left(-\frac{\bar{G} - L_t}{m}\right) \quad (2.10)$$

The parameter m is called the system characteristic load and represents the amount of additional load, in MW, that gives an LOLE that is e times greater than before, where e is the base of the system of natural logarithms. The values of B and m are typically estimated by conducting multiple LOLE calculations using equations 2.1 and 2.2 and fitting their values in the data.

The PV plant is added to the system and a fixed load is added to each hour, giving the new approximated LOLE:

$$\epsilon^{ELCC} \approx \sum_{t \in T} B \cdot \exp\left(-\frac{\bar{G} + V_t - L_t - \bar{L}}{m}\right) \quad (2.11)$$

Both equations are equated to give the ELCC:

$$\bar{L} = m \cdot \log\left(\frac{\sum_{t \in T} \exp\left(\frac{L_t}{m}\right)}{\sum_{t \in T} \exp\left(\frac{L_t - V_t}{m}\right)}\right) \quad (2.12)$$

D'Annunzio and Santoso [4] generalize Garver's approximation to multi-state generators. They focus on approximating ELCC of wind, which is multi-state since different weather condition result in different real-time output. Thus, this method can be useful in approximating ELCC for other renewables with weather-related resource constraints. It can also be applied to conventional generators, which experience different outage states. This method assumes that probabilities with which the generator being analyzed can be in different possible states is time-invariant. It relies on the same exponential risk function used by Garver that relates LOLEs to the system's

excess generating capacity. They derive the closed form capacity value for multistate generator:

$$-\frac{1}{m} \log \left[\sum_{\omega \in \Omega} \pi_{\omega} \cdot \exp(m \cdot (V_{\omega} - \bar{V})) \right], \quad (2.13)$$

to approximate the ELCC of such plants [11, 14, 7, 4].

2.2.3 Z-Method:

Z method focuses on the difference between available generating capacity and load:

$$S_t = G_t - L_t, \quad (2.14)$$

during peak hours.

Dragoon and Dvortsov [5] say that in a large power system, S , would approach a normal distribution due to the Central Limit Theorem. In these cases, LOLPs can be directly found using the Z-statistics. They also say that adding any more generators, the distribution of S remains normal. Thus, they estimate the ELCC of the generator as the load that must be added in each hour to maintain the same Z-value when the generator is added to the system. Adding a fixed load, \bar{L} , in each hour and a PV plant changes the mean and standard deviation of S_t to $\mu_S + \mu_{PV} - \bar{L}$ and $\sqrt{\sigma_S^2 + \sigma_{PV}^2}$, respectively. Thus, maintaining the same Z-statistic after the load and PV are added requires:

$$-\frac{\mu_S}{\sigma_S} = \frac{\bar{L} + \mu_S - \mu_{PV}}{\sqrt{\sigma_S^2 + \sigma_{PV}^2}} \quad (2.15)$$

Solving for \bar{L} gives:

$$\bar{L} = \mu_{PV} + Z(\sqrt{\sigma_S^2 + \sigma_{PV}^2} - \sigma_S) \quad (2.16)$$

which is simplified to:

$$\bar{L} \approx \mu_{PV} + Z \frac{\sigma_{PV}^2}{2\sigma_S}, \quad (2.17)$$

by applying a first-order Taylor approximation in σ_{PV}^2 to the radical term in equation 2.16.

The Z-method relies on the assumption that the distribution of S_t remains normal when new generators and loads are added [14].

2.3 Other Methods

There are other methods, which were proposed at a PV Capacity Workshop held during the Solar Power 2007 conference [19]. The methodologies fall into four broad categories:

1. Methodologies that measure capacity value based on the concept of loss of load probability: The Effective Load Carrying Capability (ELCC) which has already been discussed above.
2. Methodologies based on the analysis of load duration curves: Load Duration Capacity (LDC) and Demand Time Matching (DTIM).
3. Methodologies that build on the synergies that exist between short term storage/load control and PV generation: Solar Load Control Capacity (SLC) and Minimum Buffer Energy Storage Capacity (MBESC)

4. Peak-Period Capacity Factor Methodologies.

LDC: LDC is a direct analysis of the load duration curve. The LDC is defined as the mean PV output for all loads greater than a threshold defined as the utility's peak load L , minus the installed PV capacity X as illustrated in Figure 2.1, where p is the PV penetration fraction, defined as X/L .

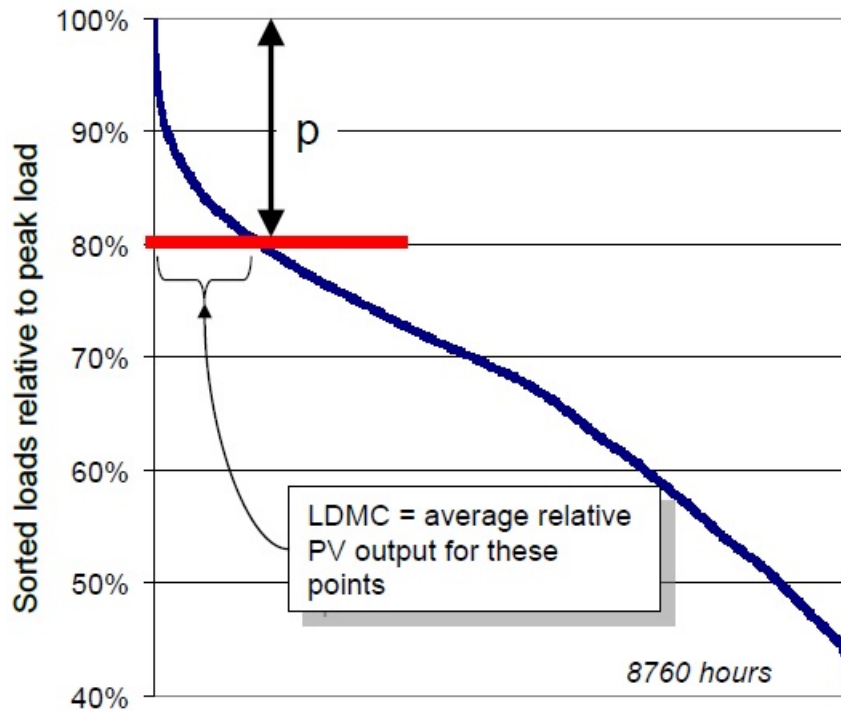


Figure 2.1: Illustration of LDC method.

DTIM: DTIM may be explained simply as the reduction in the highest net demand (i.e. demand minus available renewable capacity) when the PV is added, over a given evaluation period (Hansen [8] applies this over 10-s dispatch cycle time intervals). The capacity value is based on the worst-case difference between the load duration

curves sampled at the dispatch cycle rate over the selected evaluation period. As illustrated in Figure 2.2, the capacity value may be expressed as $DTIM = Z/X$, where $Z = (L - L')$, with L representing the highest point on the load duration curve for the evaluation period being considered and the selected sampling rate and L' representing the top of the same duration curve minus coincident PV output [6].

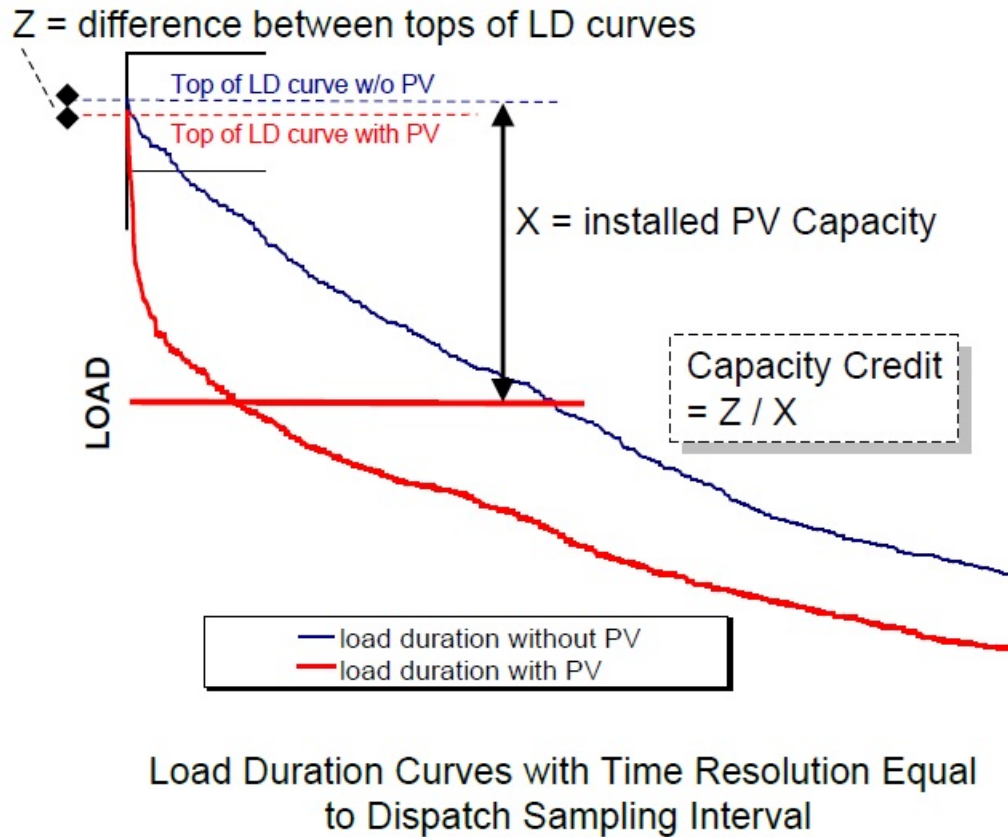


Figure 2.2: Illustration of the Demand-Time Interval Matching (DTIM) method.

SLC: The SLC metric is illustrated in Figure 2.3. SLC aims to answer the following question: Given a certain amount of Demand Response (DR) available to a utility, how much more guaranteed load reduction is possible if PV is deployed?

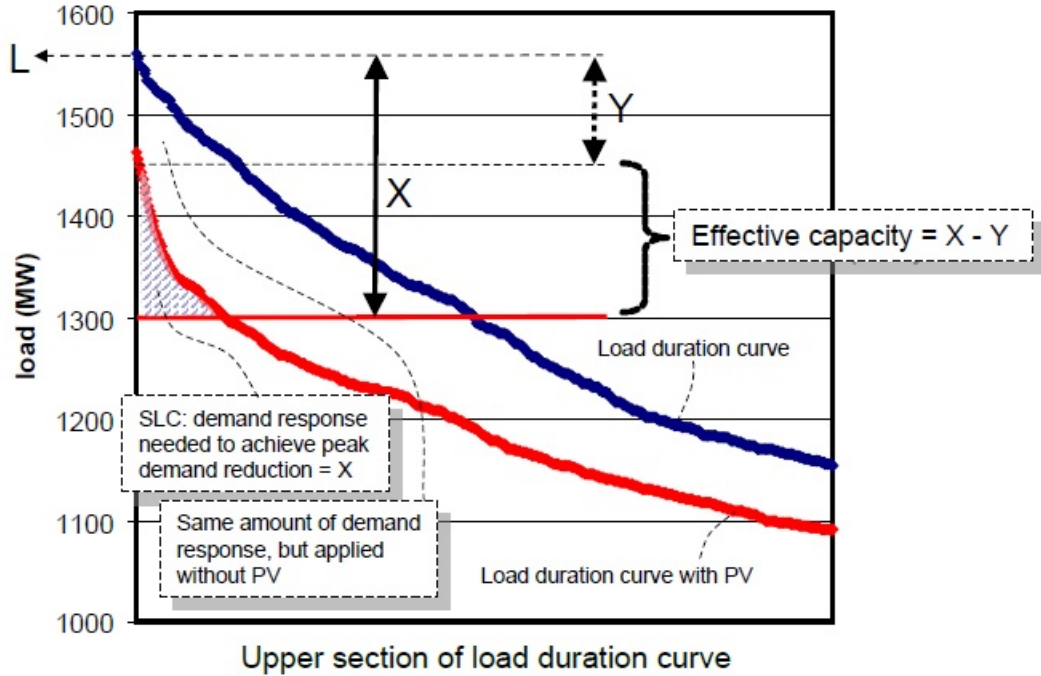


Figure 2.3: Illustration of SLC method.

Given a penetration $p = X/L$, the effective capacity is given by: $SLC = (X - Y)/X$, where Y is the amount of load reduction achieved in the absence of PV with the same cumulative amount of load control needed to guarantee a load reduction equal to X with PV.

MBESC: The MBESC metric is comparable to the SLC metric, but is determined by the storage needed to guarantee firm peak reduction the minimum buffer energy storage, MBES, concept [7, 15] - rather than cumulative DR requirements. As in the case of SLC, the metric is an answer to a certain question, in this case: Given a certain amount of dispatchable storage available to a grid or substation operator, If PV is deployed how much more guaranteed load reduction is possible? Given a PV

penetration of $p = X/L$, the method computes the minimum amount of energy storage necessary to guarantee that PV-plus-storage meets all loads above the threshold defined in the previous sections for the LDC and SLC metrics. The MBESC capacity is obtained from: $MBESC = (X - Y')/X$, where Y' is the peak load achieved using the same amount of storage but without PV. Both SLC and MBESC intend to calculate how the capacity value should vary with different penetration levels. Also these methodologies might be regarded as somewhat esoteric quantities which are associated with storage/demand response as well as the solar.

The LDC, MBESC, SLC and DTIM methods take into account the physical measure of PV penetration. They give similar approximations of capacity credit in the case study done by Hoff et al. [19] whereas the TSW metric which does not take into account the effect of PV penetration provides a considerably different measure of capacity credit.

Chapter 3: Case Studies

A summary of several case studies are presented in this section. Most of these studies are based on methodologies described in Chapter 2.

Madaeni et al. [14] compare the capacity value estimation techniques for photovoltaic solar power. They take 14 locations in the WECC footprint for their analysis. They use 100 MW nameplate capacity PV power plants for their analysis. The ELCCs are in the range of 52% to 70% and their ECPs are in the range of 56% to 75%. The ELCCs are lower because the PV is benchmarked against a generator with a positive EFOR in the ECP method. In the ELCC method, PV is compared to a constant load which is similar to a fully reliable generator with a 0% EFOR. Their analysis uses the same load pattern for all locations so the different capacity values are solely due to regional variations in the solar resource across the locations. They also show how generation during peak hours has a direct impact on capacity value by taking the example of PV in Los Angeles, which has a lower capacity value than that in Congress, AZ because the PV generation is more coincident with the loads than the generation in Los Angeles. Here the correlation between local loads and PV generation is not captured as the analysis takes the WECC-wide footprint for their loads. They also study the interannual variation in capacity values between the

years studied. The ECP of PV in Congress, AZ varies from 48% in 1999 to 85% in 2002. This is explained by variable solar availability patterns from year to year. This is also due to the PV output being less coincident with the load pattern in 1999. This indicates that several years of data are required for a robust analysis. They also compare the ELCC and ECP analysis with the approximation based methods. The paper finds that the capacity factor based method is most accurate. The other methods also give close approximation of capacity values.

Pelland and Abboud [18] study the photovoltaic capacity values for the city of Toronto. They calculate capacity factor using Garver approximation for loads within a given percentage deviation from the peak and they also calculate capacity factor during summer peak time. They conduct their analysis for the years 2000-2006 and for a grid penetration level of 2%, 5%, 10% and 20%. They also study the effects of orientation of PV in southerly, southwesterly, and westerly directions. Using the Garver approximation, they find that the capacity value decreases as the grid penetration increases. The best capacity value was found for a 2% grid penetration level. In their second method, for the peak loads, the SW and W orientation give higher mean PV outputs than the S orientation, which has a higher yearly capacity factor. The mean PV output over hours within 10% of the peak is found to be approximately 35% for all orientations. The mean PV values by method 3 for summer period between 11am 5pm are around 43% for all orientations. The approximate capacity values in this paper are within the range of PV capacity values as computed in other analyses [14, 20].

Perez and Hoff [10] conduct energy and capacity valuation of photovoltaic power generation in New York for Solar Alliance and The New York Solar Energy Industry Association. Their results also show that the capacity credit of PV in New York is high but it decreases with increasing grid penetration. One of the regions (Long Island) has greater resilience of capacity credit at high penetration because it is highly summer peaking. A similar analysis is carried out for PV capacity values in Minnesota [12]. The results are similar to the NY analysis. Perez et al. [21] also conduct a US-wide utility analysis to calculate PV capacity by ELCC. The PV in the southwestern US exhibits the highest capacity values, followed by PV in the Central US and mid-Atlantic regions. The lowest ELCCs are found in the North Pacific coast, the northern fringes of the Great Lakes and New England, and to a lesser extent, Florida. The Perez et al. study provides considerably more insight on the effects of PV penetration. With fixed optimized PV arrays, the national average for ELCC at low penetration is nearly 55%, reaching 65%+ in the best cases. ELCC erodes down to $\sim 35\%$ nationwide at 20% penetration reaching 45% in the best cases.

Hoff et al. [9] conduct ELCC calculations for PV generation in Austin, Texas. They study the effects of different types of PV systems (1-axis tracking and fixed axis) with different orientations and angles. Their ELCCs are in the range of 30% - 65% and the best result is for a single-axis system with a 30 degree tilt. Similar kind of sensitivity analysis is done by Madaeni et al. [14], who find that capacity values with single-axis and double-axis tracking are higher than fixed-axis PV.

Perez et al. [19] carry out case studies to examine the effectiveness of the other methods described in Section II. Three utilities are examined - Nevada Power (NP), Rochester Gas & Electric (RG&E) and Portland General (PG) for the case studies and one year of load and PV generation data are analyzed for each. All the methodologies are applied to the data and the results from each methodology are compared. It is found that for all the methodologies that are based on a physical measure of PV penetration (ELCC, LDMC, MBESC, SLC and DTIM), all measures of capacity value are comparable (when comparing capacity value metrics as a function of PV penetration). However methodologies that are based on defining a peak demand time frame lead to different results [6].

Chapter 4: Data and Model

In this study, we estimate the capacity value of PV at 10 sites spread across the United States. These sites are chosen to represent a mix of locations that have summer peaking loads, winter peaking loads, good/bad solar resource, and availability of both measured and modeled solar data. The capacity value is estimated for hourly as well as subhourly PV and wind for years from 1998 to 2013 contingent upon availability of conventional generator, load, and solar data at these locations. Our analysis considers small 100 MW PV plants at each location. Our capacity value estimates are for marginal PV installations and do not account for the diminishing marginal capacity value that occurs with higher PV penetration. The capacity value at these locations are computed in isolation, thus avoiding spatial correlation of solar availability between locations that may occur otherwise.

4.1 Photovoltaic Data and Model

There are 2 types of solar data sources chosen in our study one in which solar data are actually measured on the ground physically and the other in which the solar data are modeled using satellite data. Measured solar data sources are the ‘surfrad’ and ‘mide’ whereas ‘nsrdb’ is the modeled data source.

Table 4.1: Location information

Location	Coordinates	Years
Nevada Energy, Nevada (NE)		
1	36.09N -115.07W	2006
2	36.09N -115.15W	2006
3	36.61N -116.03W	1992-2002, 2004-2013
Public Service Company Colorado, Colorado (PSCC)		
4	39.74N -105.18W	2005-2006
5	40.13N -105.23W	1999-2002, 2004-2013
NorthWestern Energy, Montana and South Dakota (NWE)		
6	48.33N -105.11W	1998-1999, 2002-2005, 2007-2013
7	43.73N -96.63W	1998-1999, 2002-2003
Southern Mississippi Electric Power Association, Mississippi (SMEA)		
8	34.25N -89.87W	1998-2013
Southern Illinois Power Cooperative, Illinois (SIPC)		
9	40.05N -88.39W	1998-2007
West Penn Power, Pennsylvania (WPP)		
10	40.73N -77.95W	1999, 2002-2003, 2007-2013

PV generation is modeled using PVWatts version 5 of the National Renewable Energy Laboratory’ Solar Advisory Model (SAM) Software Development Kit (SDK). This model takes weather data, including solar irradiation, temperature, and wind speed as inputs and simulates hourly net AC electrical output of a PV plant. It accounts for losses and other parasitic loads. Our analysis assumes fixed-axis PV panels oriented southward with an azimuth angle of 180 and a tilt angle equal to the site’s latitude.

4.2 Conventional Generators

Each generator’s rated capacity is obtained from Form 860 data filed with the United States Department of Energy’s Energy Information Administration (EIA). We estimate EFORs of the existing generators using the North American Electricity

Reliability Corporation’s Generator Availability Data System (GADS). The GADS specifies historical annual average generator EFORs based on capacity and technology. We combine this with EIA Form 860 data, which specify generator prime mover and generating fuel, to estimate EFORs, average generating capacity and number of generating units. We do this for each utility, based on the PV site location.

Generator outages are modeled using the EFORs. LOLPs are estimated by computing the system’s capacity outage probability table (COPT). In this table, all combinations of available and unavailable generating units are presented in tabular form with the calculated system availability.

4.3 Load Data

Hourly historical load data for each year are obtained from Form 714 filings with the Federal Energy Regulatory Commission (FERC). The FERC data include reports for nearly all of the load-serving entities and utilities. We consider the loads of only a subset of these utilities which operate in the region of our PV sites. Each hourly load is repeated 60 times to get the load data in subhourly format. Since the system loads and conventional generation capacity vary over the study period, we adjust the hourly load profiles in each year individually so that the LOLPs of the base system in each year sum to 144. This corresponds to the standard planning target of one outage-day every ten years. This load adjustment is done by scaling all of the hourly loads by a fixed percentage ranging between 0.01% and 5% in the different years.

Table 4.2: Utility load data (GW)

Utility	Average	Summer Peak	Winter Peak
NE	1.9-3	4-6.3	2.2-4
PSCC	2.8-4.8	4.5-8.2	4.0-6.8
NWE	0.3-1.1	0.4-1.5	0.4-1.5
SMEA	0.2-1.7	0.2-2.7	0.4-2.9
SIPC	1.8-5.5	3.2-9.4	2.5-7.2
WPP	4.5-8.1	6.4-13.8	6.8-10.9

4.4 Example: Compute ELCC of 35 MW Solar PV plant

Suppose there are two conventional generators in the model - 2 units of 20 MW capacity with an EFOR of 0.1 and 1 unit of 30 MW capacity with EFOR of 0.2 as given in table 4.3.

Table 4.3: Example: conventional generators available

Capacity (MW)	20	30
Units	2	1
EFOR	0.1	0.2

The COPT for these generators is explained by table 4.4

Table 4.4: Example: Capacity Outage Probability Table (COPT)

Capacity Out	Capacity In	Prob of Cap In	Cumulative Prob
70	0	$0.1^2 * 0.2 = 0.002$	0.002
50	20	$2 * 0.9 * 0.1 * 0.2 = 0.036$	0.038
40	30	$0.8 * 0.1^2 = 0.008$	0.046
30	40	$0.2 * 0.9^2 = 0.162$	0.208
20	50	$2 * 0.9 * 0.8 * 0.1 = 0.144$	0.352
0	70	$0.8 * 0.9^2 = 0.648$	1

After we get the COPT table, base case **LOLE** is computed using equation 2.1 and 2.2 as shown in table 4.5.

Table 4.5: Example: LOLE computed for the base case

L_t	LOLP
16	0.002
24	0.038
30	0.038
41	0.208
56	0.352
68	0.352
76	1
67	0.352
40	0.046
32	0.046
26	0.038
5	0.002
LOLE (ϵ)=	2.474

Once we get the base case LOLE, the **ELCC** of 35 MW solar PV plant is computed by changing \bar{L} iteratively such that ϵ^{ELCC} is equal to ϵ as given in equation 2.4. This is computed in table 4.6.

Table 4.6: Example: ELCC computed for 35 MW solar PV plant

L_t	PV_t	$L_t - PV_t + \bar{L}(16)$	LOLP
16	0	32	0.046
24	0	40	0.046
30	5	41	0.208
41	15	42	0.208
56	25	47	0.208
68	30	54	0.352
76	35	57	0.352
67	22	61	0.352
40	12	44	0.208
32	2	46	0.208
26	0	42	0.208
5	0	21	0.038
		LOLE (ϵ^{ELCC})=	2.434

Chapter 5: Results: Case Study across North America - Solar PV

We use the ELCC metric described in Chapter 2 to compute the capacity value of solar PV plants in our study for 10 locations as given in table 4.1. The first two locations in Nevada have only mean absolute difference because ELCC is estimated only for one year.

The ELCCs estimated using hourly solar data are compared with the ELCCs estimated using subhourly solar data in table 5.1. The ELCCs in this table are averaged over the years for that particular location. We see that there is an absolute difference as high as 8.2% between the ELCCs computed using hourly and subhourly data for PV plant located in Nevada. This difference is only for one year and as we have higher number of years in our analysis, the average smooths out. The maximum difference in ELCC goes upto 16% for PV plant situated in Montana in the year 2005, which shows that using hourly solar data can introduce significant errors in estimating ELCCs for a particular year.

We compare the ELCCs computed using the original load data with ELCCs computed using load data shifted one hour ahead and one hour behind. This is to see if ELCCs are sensitive to the sloppiness in the reported load data. This is summarized in table 5.2. Positive difference means ELCC estimated using shifted load is higher

Table 5.1: Average Hourly and Subhourly ELCCs and Absolute Value of Differences in ELCCs Estimated Using Hourly and Subhourly Solar Data

Location	Hourly ELCC	Subhourly ELCC	Mean Difference		Maximum Difference	
			MW	%	MW	%
1	31.10	30.40	0.70	2.30		
2	28.40	26.25	2.15	8.20		
3	24.46	24.21	0.26	1.25	1.65	9.27
4	24.30	23.10	1.2	5.04	1.60	5.97
5	24.48	24.19	0.33	1.33	1.00	2.42
6	16.49	16.60	0.43	2.23	3.56	15.51
7	12.67	12.35	0.32	3.94	0.47	9.87
8	25.66	25.53	0.17	0.64	0.45	1.51
9	27.21	26.98	0.30	1.13	1.40	4.98
10	21.16	20.94	0.22	1.07	0.46	2.89

compared to ELCC estimated using the original load. For all the locations, shifting the load one hour back gives an average increase in the ELCC estimates, whereas shifting the load one hour forward gives a decrease in the ELCC estimates. The error in ELCC estimates is more than 30% in certain cases which shows that ELCCs are highly sensitive to the interpretation of load data.

We also compare the ELCCs estimated using measured and modeled solar radiation data. The table 5.3 shows that modeled solar data can introduce significant errors in ELCC estimates. A positive difference means that ELCC estimated using modeled data is higher than the ELCC estimated using measured data. The first two locations only have the average difference because the ELCC were estimated for a single year. From the results, we see that the maximum error in certain cases such as PV located in Mississippi and Pennsylvania can go up to 104% and 71% respectively,

Table 5.2: Average Differences in ELCCs Estimated Using Load Shifted One Hour Backward and Forward One Hour and Original Load Data

Location	Shifted Backward		Shifted Forward	
	Difference	Abs Value	Difference	Abs Value
1	31.32	31.32	-31.38	31.38
2	29.64	29.64	-30.38	30.38
3	41.61	41.61	-37.17	37.17
4	36.85	36.85	-34.66	34.66
5	34.59	34.59	-31.59	31.59
6	3.10	6.76	-4.16	7.23
7	30.12	30.12	-29.25	29.25
8	16.19	20.81	-17.58	21.75
9	17.93	17.93	-19.85	19.85
10	4.68	5.35	-5.01	9.77

which shows that ELCC estimates using modeled solar radiation data may not give accurate results. We have excluded years which have missing data for measured solar radiation. Missing data may be due to possible instrument or data recording failures.

Table 5.3: Average, Maximum and Minimum Difference in ELCC Estimates using Measured and Modeled Solar Radiation Data.

Location	Average	Minimum	Maximum
1	-1.13		
2	10.42		
3	-20.92	11.78	-42.18
4	3.18	4.95	1.41
5	-0.63	21.09	-24.02
6	-5.97	41.20	-27.27
7	24.43	48.02	6.10
8	13.04	104.17	-10.40
9	8.24	33.91	-0.62
10	20.49	71.01	7.85

Depending on location, the ELCC of PV can range between 5 MW and 42 MW which corresponds to 6% and 50% of the 83 MW ac nameplate capacity of the PV plants studied. The ELCC values are lower compared to the study by Madaeni et al. [14]. This may be due to the fact that Madaeni et al. consider load for the entire WECC footprint whereas here, load is considered in smaller regions. Thus, the difference in ELCC between the locations is primarily due to differences in the coincidence between PV generation and system loads. It is known from past studies that capacity value largely depend on the amount of PV generation during the peak load time of the day, and PV generation during high load days of the year [14, 19, 22].

Some of the results for the following cases are explained using visuals for PV generation and load profiles for time of the day and highest load days of the year:

1. Comparison of ELCCs computed using the measured hourly and subhourly data.
2. Comparison of ELCCs computed after shifting loads 1 hour ahead and back.
3. Comparison of ELCCs computed using measured solar and modeled solar data.

5.1 Comparison of ELCCs computed using hourly and sub-hourly solar data

In power system planning, the norm has been to estimate capacity value using hourly data. Solar and other renewables which have uncertain real-time output due to weather conditions can be sensitive to minute based changes in weather. In this section, by comparing ELCC estimates using hourly and subhourly solar data, we want to see if the ELCC estimates using hourly solar data is as accurate as the ELCC estimates using subhourly data.

The result for the difference in capacity value estimates using hourly and subhourly solar radiation data are summarized in table 5.1.

Our results show that for some locations, ELCC computed using hourly data overestimates ELCC computed using subhourly data. For example, PV located in Nevada (36.09, -115.15), in the year 2006 has loads peaking late in the day when hourly PV generation is higher compared to subhourly PV generation. This can be seen in Fig 5.1. The highest load day, which is on 18th July, has a higher hourly PV generation during the peak load times of the day compared to subhourly PV generation (5.2) explaining the overestimation of ELCC computed using hourly data compared to ELCC computed using subhourly data.

In some cases, such as a PV plant located in Montana (location 6), in the year 2005, ELCC calculated using hourly solar radiation underestimates the ELCC compared to ELCC using subhourly solar radiation. From Fig 5.3, we can see that subhourly solar radiation data gives a higher average PV output. Also, The highest load day for MPC, which is the utility in that region, is on 13th July. The PV output and load graph (Fig 5.4) on that day shows that subhourly PV has a higher average PV

output compared to the hourly PV output. This explains the underestimation of ELCC computed using hourly data compared to ELCC computed using subhourly data.

There are other cases, such as a PV plant located in Nevada (36.61, -116.03) which give negligible or zero difference between the ELCCs computed using hourly data and ELCCs computed using subhourly data for the year 2007. As seen from Fig 5.5 and Fig 5.6, the hourly PV output and subhourly PV output overlap. This explains the zero difference between ELCC estimated using hourly and subhourly data.

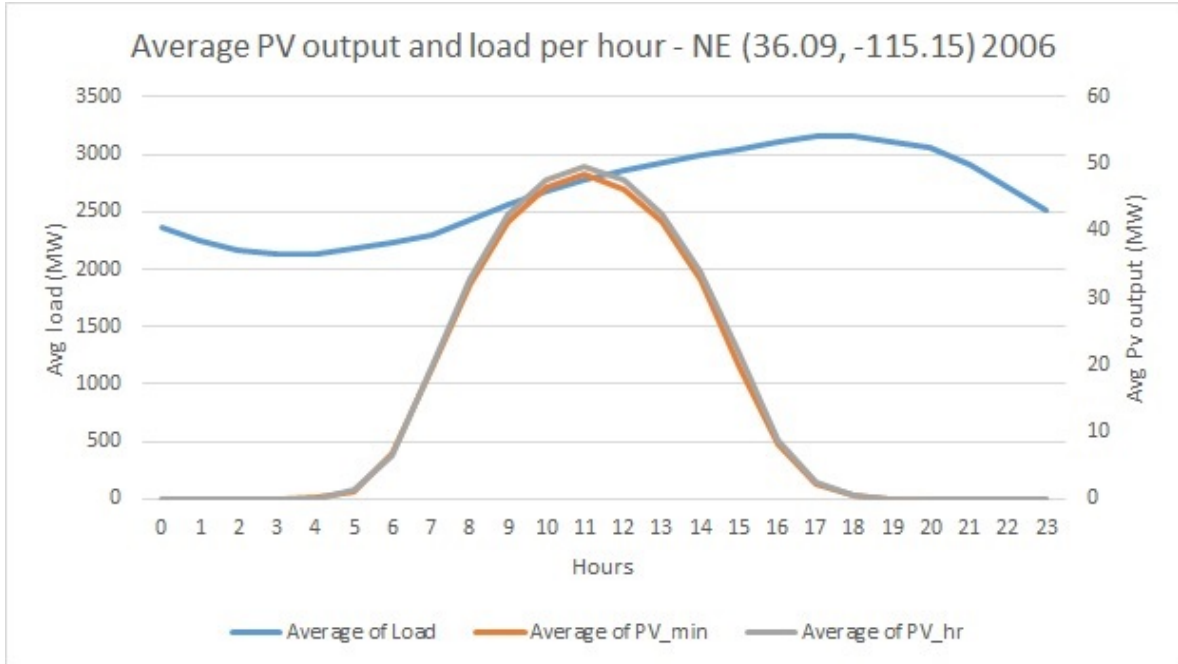


Figure 5.1: Nevada(2006) - Average load, average hourly PV output and average minute based PV output for hours of the day for all the days of the year.

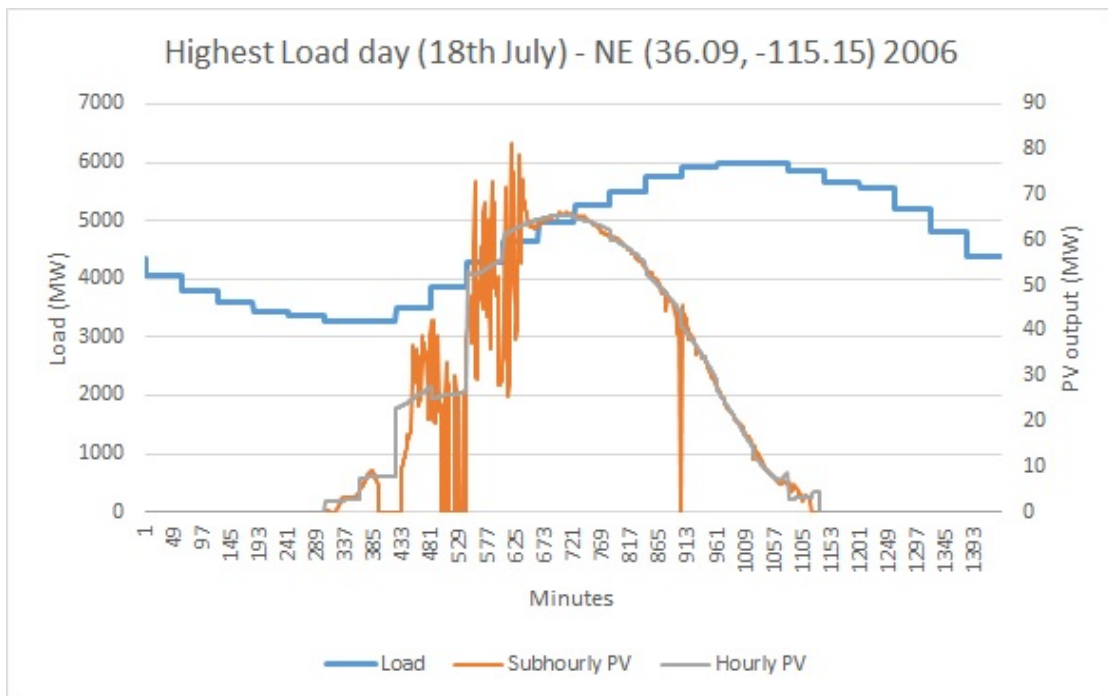


Figure 5.2: Nevada(2006) - Load, hourly PV output and subhourly PV output on the highest load day.

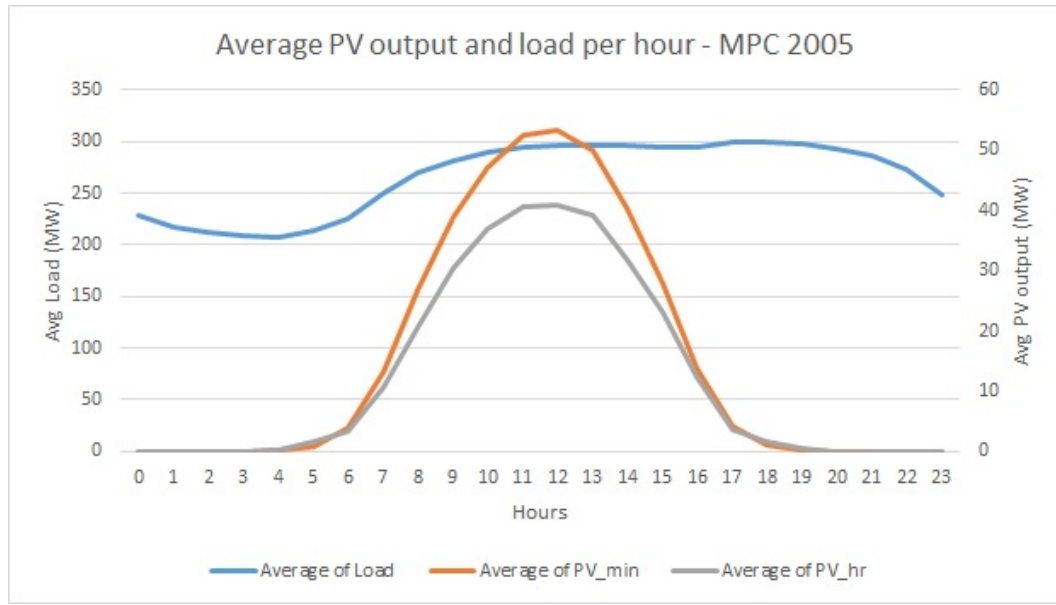


Figure 5.3: Montana(2005) - Average load, average hourly PV output and average minute based PV output for hours of the day for all the days of the year.

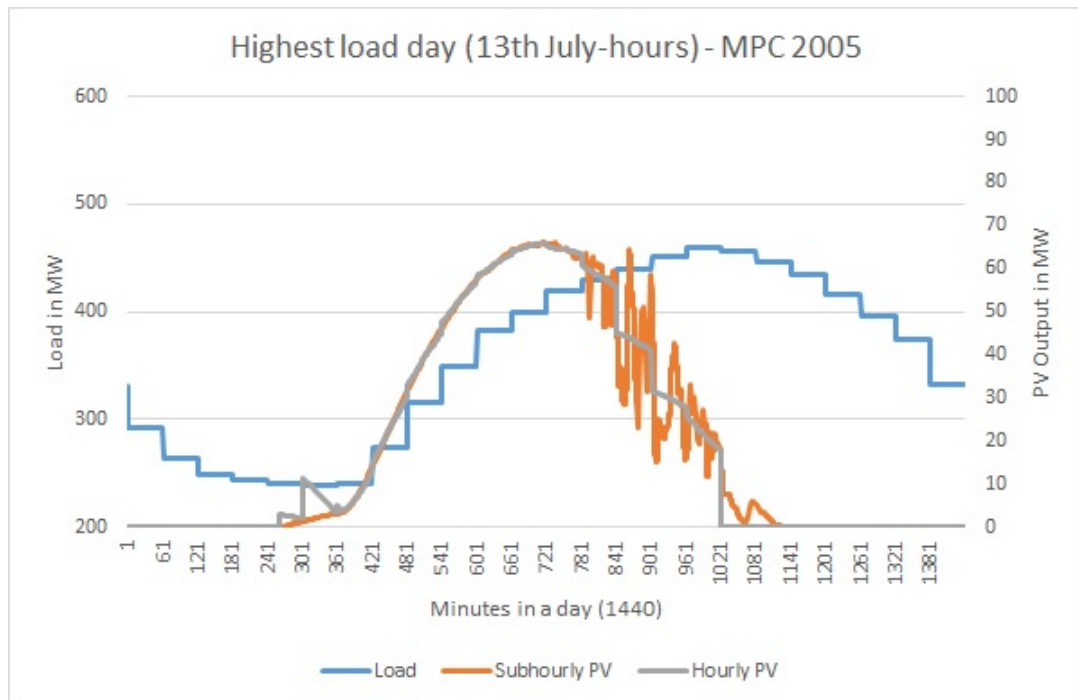


Figure 5.4: Montana(2005) - Load, hourly PV output and subhourly PV output on the highest load day.

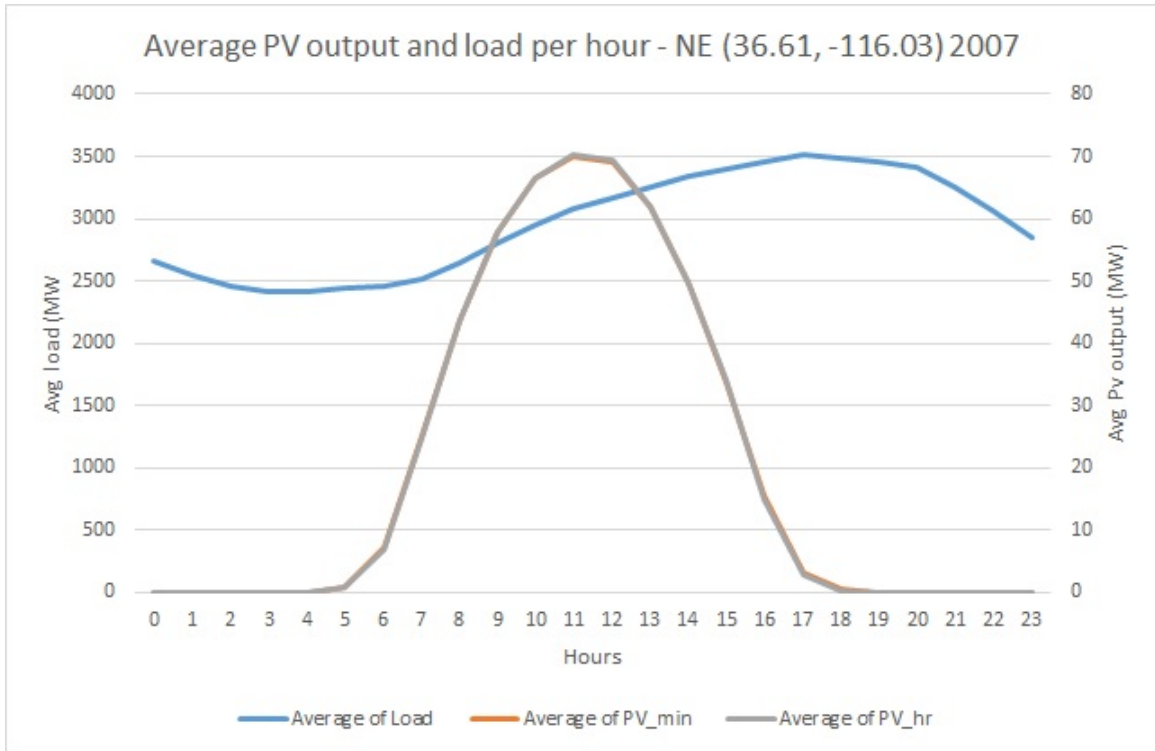


Figure 5.5: Nevada(2007) - Average load, average hourly PV output and average minute based PV output for hours of the day for all the days of the year.

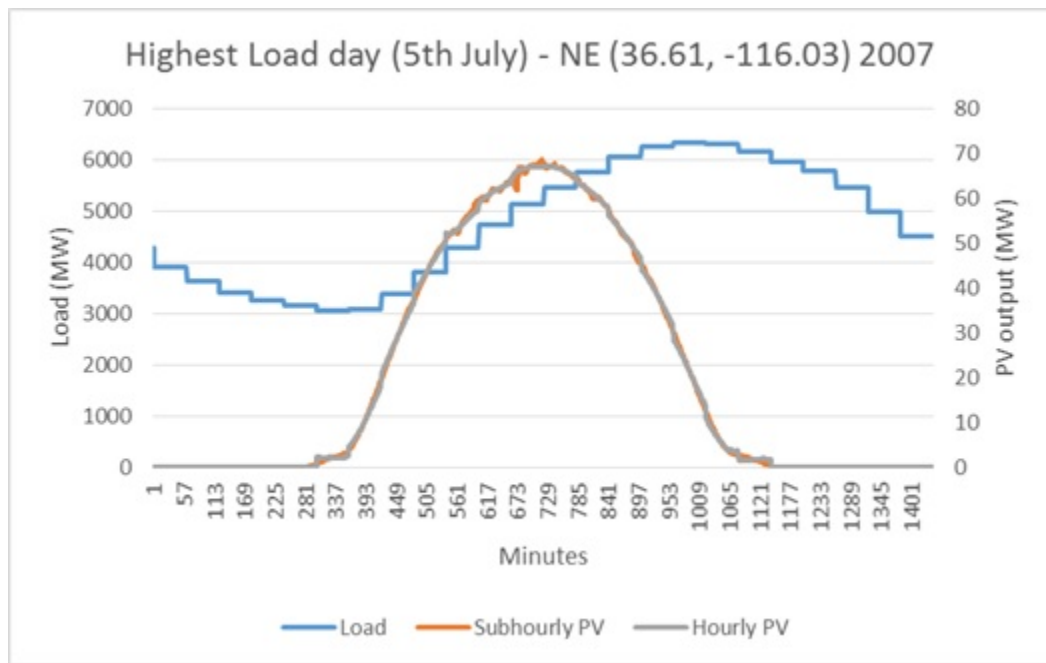


Figure 5.6: Nevada(2007) - Load, hourly PV output and subhourly PV output on the highest load day.

5.2 Comparison of ELCC computed using original load data and ELCC computed after load data is shifted one hour ahead and behind

The load data is reported in hourly intervals. The question is whether this load is instantaneous at that hour or is it the average of the previous hour or is it the average of the next hour? The other major question is whether the data reported takes into account day light saving times. We want to know how sensitive ELCC estimation is to sloppiness of the reported load data. We can see this by computing ELCCs after shifting the load data one hour ahead and one hour behind and compare it with the ELCC computed using original reported load data. The results are summarized in Table 5.2. A few worst case scenarios are explained in this section.

With the summer peaking loads, for example consider a PV plant location in Nevada (36.61, -116.03). The peak load occurs on 24th August. Also, the loads peak late in the day when it is hot and sunny. During this time, the PV output is high as well. When the load is shifted one hour behind, there is more PV output giving a higher ELCC compared to ELCC computed without shifting the load. When the load is shifted one hour ahead, the load peak occurs later in the day when the PV output is lower as seen from Fig 5.7 and 5.8, thus giving lower ELCC compared to ELCC computed without shifting the load.

For cases where peak loads occur early in the day, ELCC of PV plant is underestimated when computed using load shifted one hour behind and overestimated when computed using load shifted one hour ahead. We take the case of ELCC of PV plant located in Mississippi (34.25, -89.87) for the year 2003. When the load is shifted an hour ahead, there is higher PV output during the peak load compared to when the

load is shifted an hour behind (Fig 5.9). This observation is reiterated in the peak load day for the same utility in 2003 (Fig 5.10).

It is interesting to note that load curve is not specific to location but it varies from year to year as well. Like in the case of Mississippi and Montana, the load curves vary from year to year which makes it a summer peaking system during some years whereas a winter peaking system during the others. Thus, we have ELCCs which are either overestimated or underestimated by shifting the loads one hour ahead or one hour behind.

There are also certain cases where there is negligible difference in the ELCC computed using load shifted one hour ahead or one hour behind. This may occur when the load is almost constant throughout the day, especially when there is PV generation. This happens for a case in Pennsylvania (40.73, -77.95). As we see from Fig 5.11, the load lines are overlapping each other at the time of PV generation. Considering the highest load day, which occurs on 16th Jan, we can see that there is negligible change in the load plots after shifting the loads (Fig 5.12). This explains the negligible difference in ELCC computed using the shifted load data and ELCC computed using the actual load data.

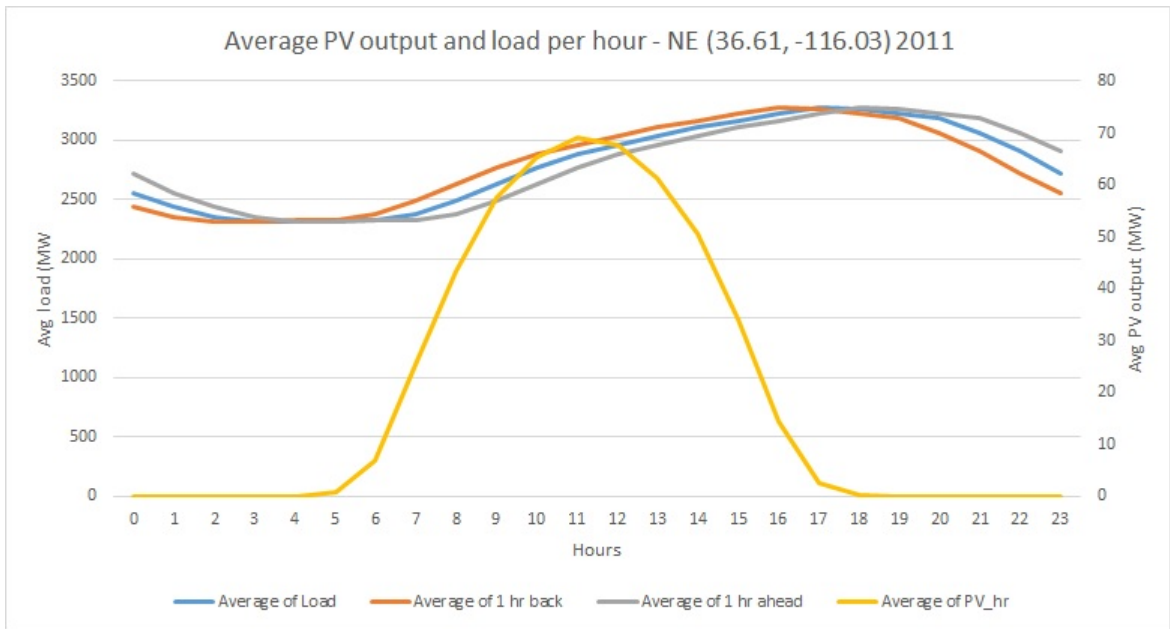


Figure 5.7: Nevada(2011) - Average load, average load shifted 1 hour back, average load shifted 1 hour ahead and average hourly PV output for hours of the day for all the days of the year.

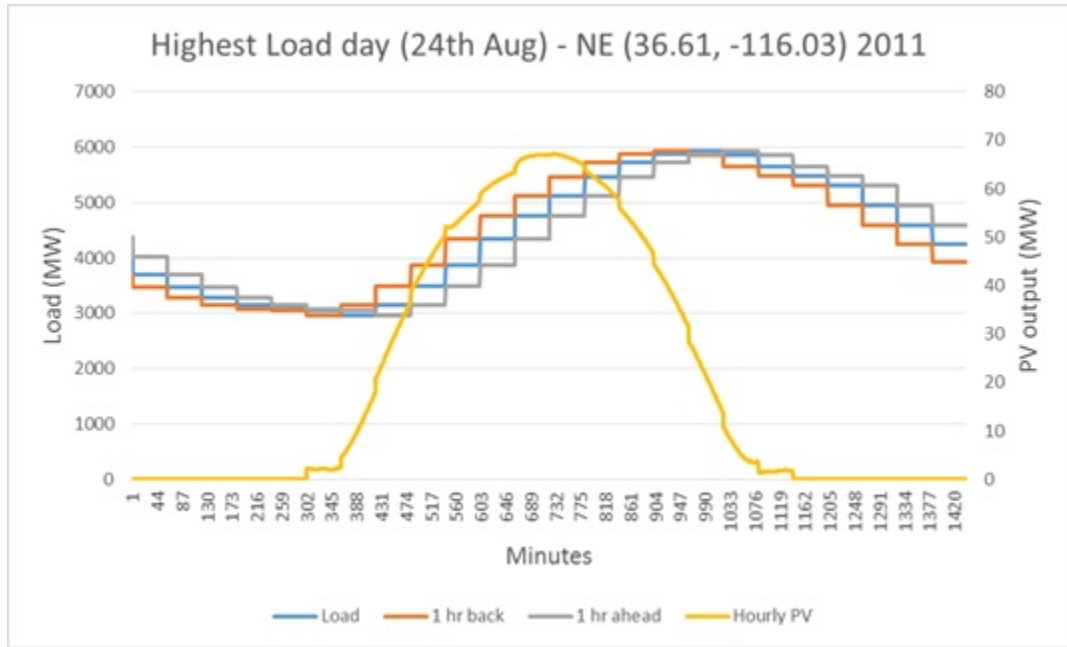


Figure 5.8: Nevada(2011) - Load, load shifted 1 hour back, load shifted 1 hour ahead and hourly PV output on the highest load day.

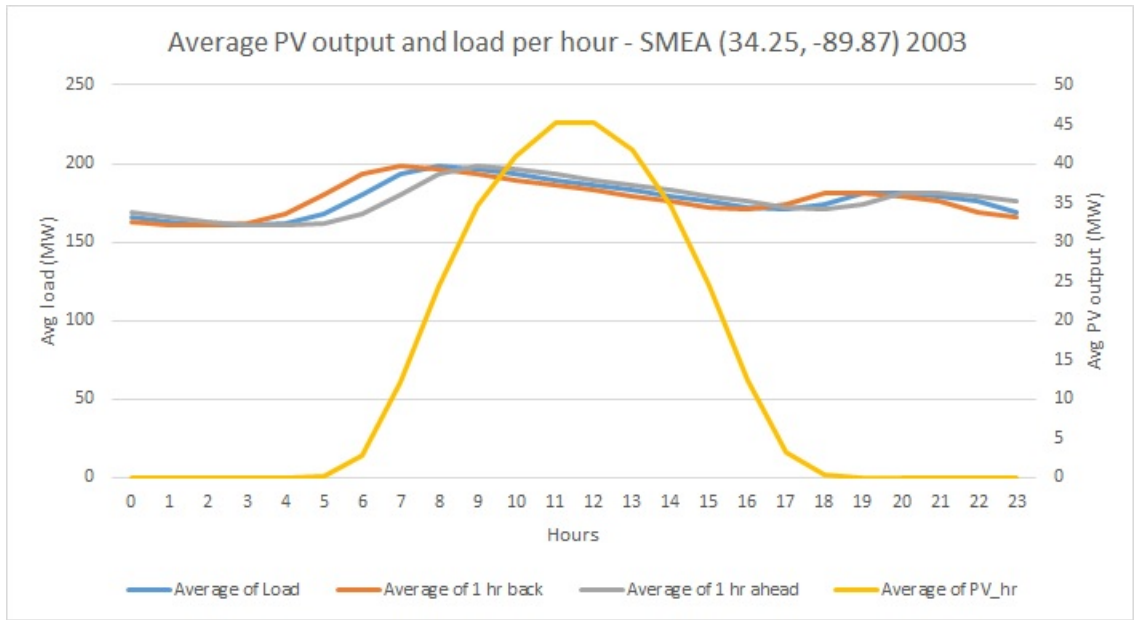


Figure 5.9: Mississippi(2003) - Average load, average load shifted 1 hour back, average load shifted 1 hour ahead and average hourly PV output for hours of the day for all the days of the year.

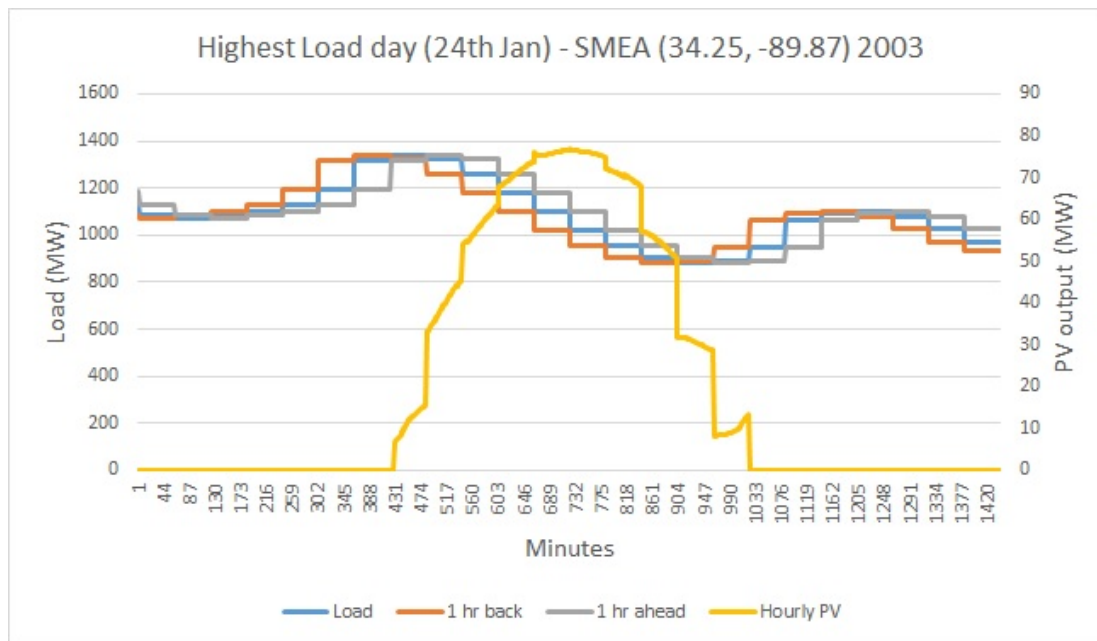


Figure 5.10: Mississippi(2003) - Load, load shifted 1 hour back, load shifted 1 hour ahead and hourly PV output on the highest load day.

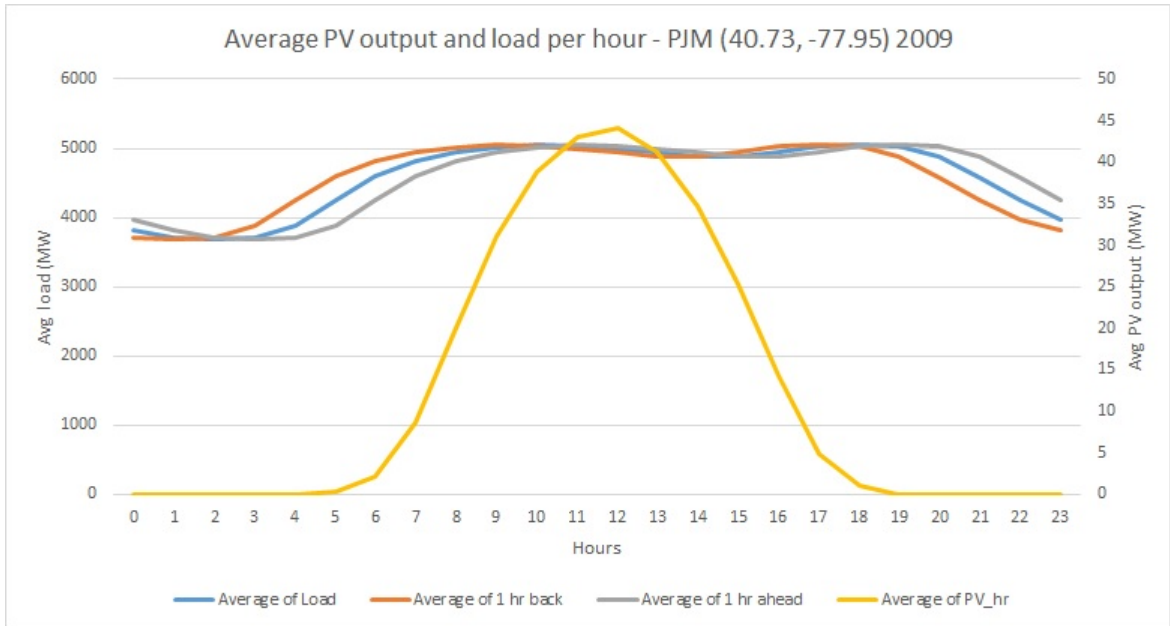


Figure 5.11: Pennsylvania(2009) - Average load, average load shifted 1 hour back, average load shifted 1 hour ahead and average hourly PV output for hours of the day for all the days of the year.

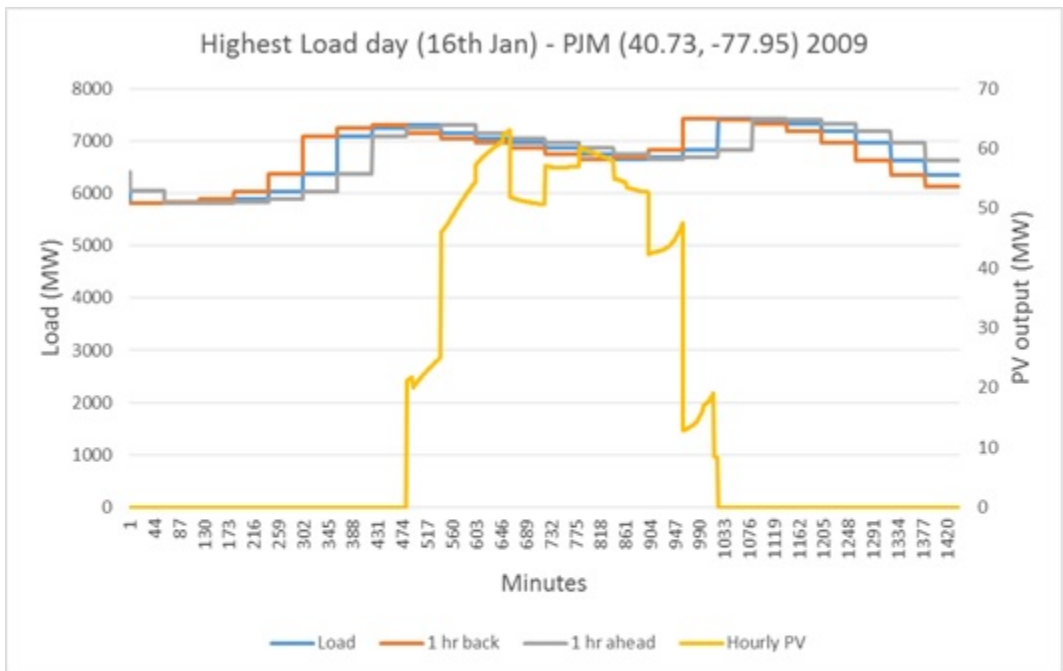


Figure 5.12: Pennsylvania(2009) - Load, load shifted 1 hour back, load shifted 1 hour ahead and hourly PV output on the highest load day.

5.3 Comparison of ELCC computed using measured (surfrad) data and ELCC computed using modeled (nsrdb) data

The access to satellite data, which is the modeled data is for locations on a $4km^2$ grid across North America. It is difficult and expensive to get real-time measured data for these many locations. Thus, we want to see if the modeled data does justice to the ELCC estimation. To do so, we compare the ELCCs estimated using actual measured (surfrad) solar data and ELCCs estimated using modeled (nsrdb) solar data and explain the findings in this section. Table 5.3 summarizes the results.

From the result, we can see that cases such as a PV plant located in Nevada (36.61, -116.03) in the year 2012, overestimates ELCC when computed using measured data. It is seen from Fig 5.13 that the measured data has higher average output than the modeled data when the load peaks. The measured data has higher PV output on the highest load day which explains the overestimation of ELCC computed using measured data This is clearly shown in Fig 5.14.

Cases, such as a PV plant located in Mississippi (34.25, -89.87) for the year 2013 underestimate ELCC computed using measured data. Modeled data has a higher PV output than the measured data during the high load times of the day as seen in Fig 5.15. Looking at the highest load day of the year (Fig 5.16), we can see that measured data has a higher PV output but this output is during the time of the day when the load is lower. Modeled data has a higher output during the higher load times of the day. This can explain the underestimation of ELCC computed using measured data compared to ELCC computed using modeled data.

We get a few cases where the ELCC computed using measured and modeled data show no difference. One such example is for PV located in Colorado (40.13, -105.23)

for the year 2009. From Fig 5.17, we can see that though the average PV output for measured solar data is higher than the average PV output for modeled solar data, the peak PV output for measured solar data is during the time when load is low. The PV output during the highest load day for measured data and modeled data is almost coincident in Fig 5.18. This can explain the same ELCC estimation computed using both these data sets.

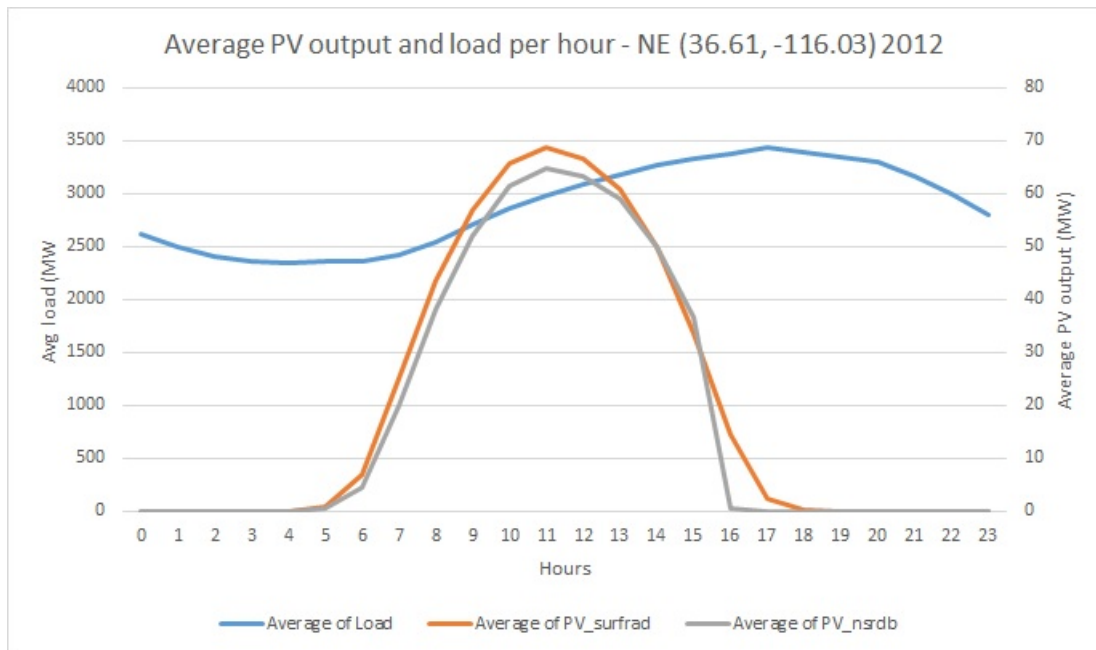


Figure 5.13: Nevada(2012) - Average load, average PV output from measured and modeled radiation data for hours of the day for all the days of the year.

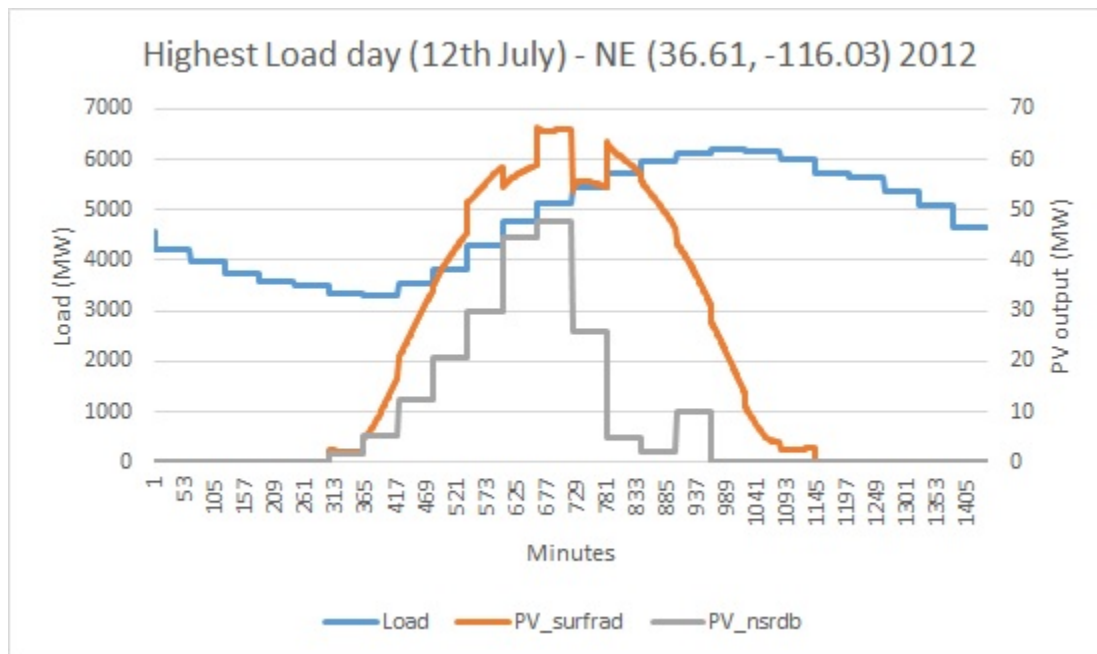


Figure 5.14: Nevada(2012) - Load and PV output on the highest load day.

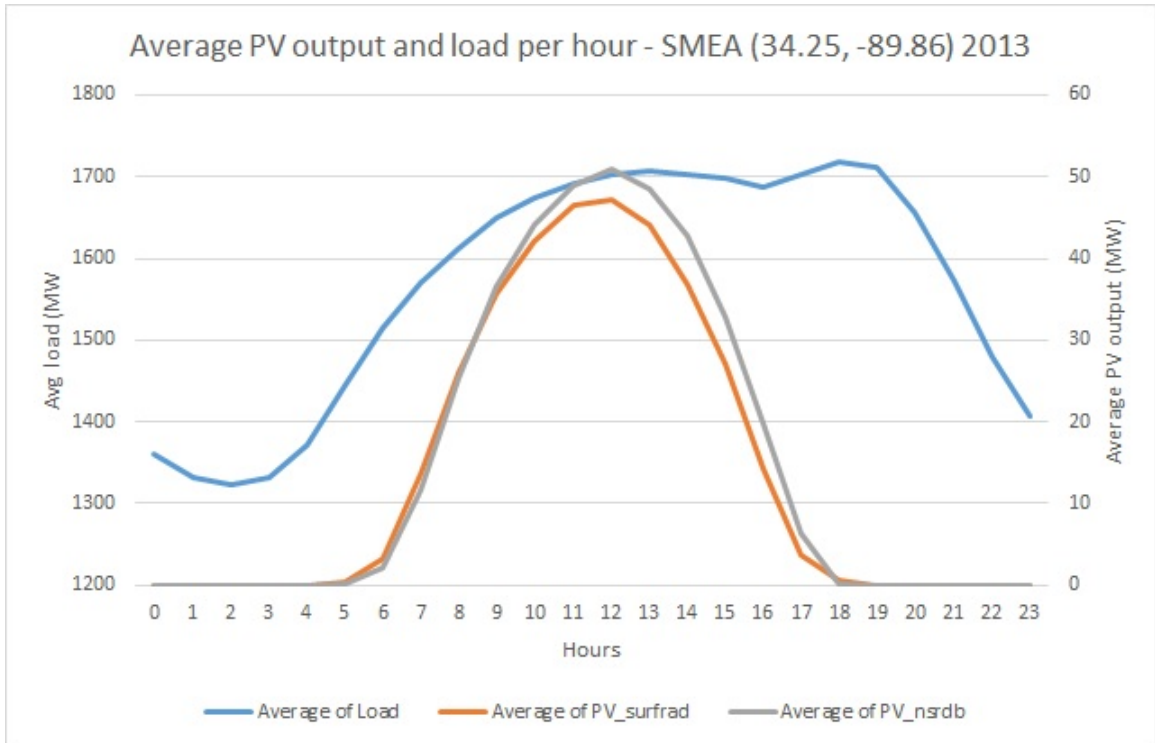


Figure 5.15: Mississippi(2013) - Average load, average PV output from measured and modeled radiation data for hours of the day for all the days of the year.

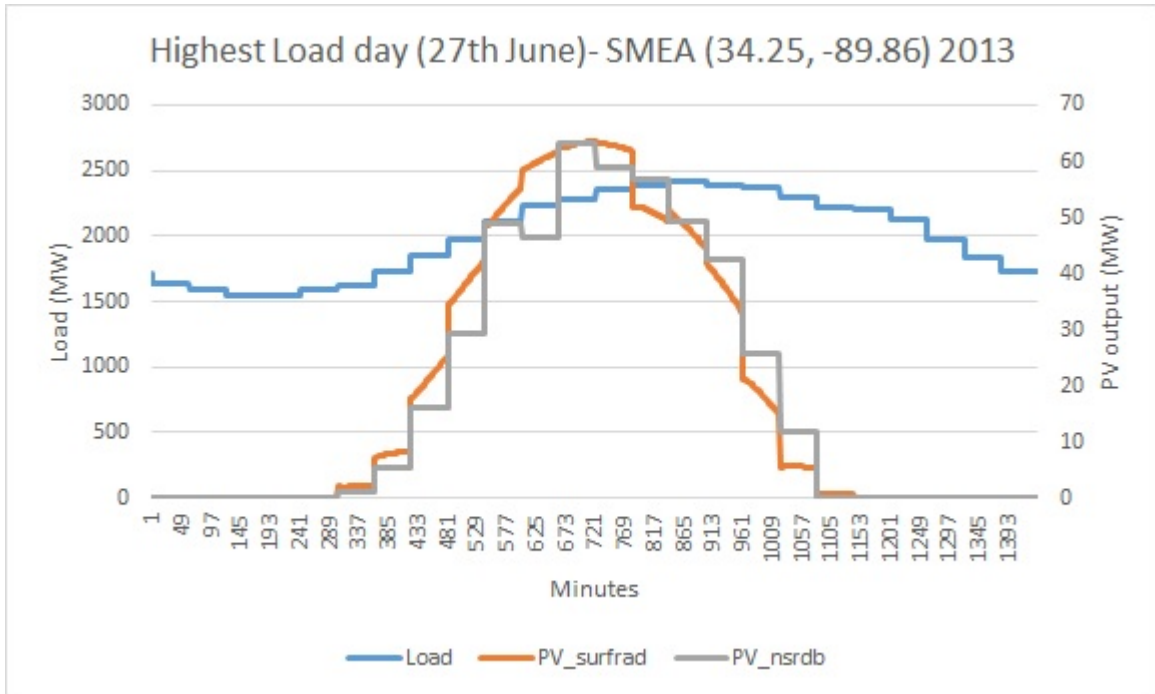


Figure 5.16: Mississippi(2013) - Load and PV output on the highest load day.

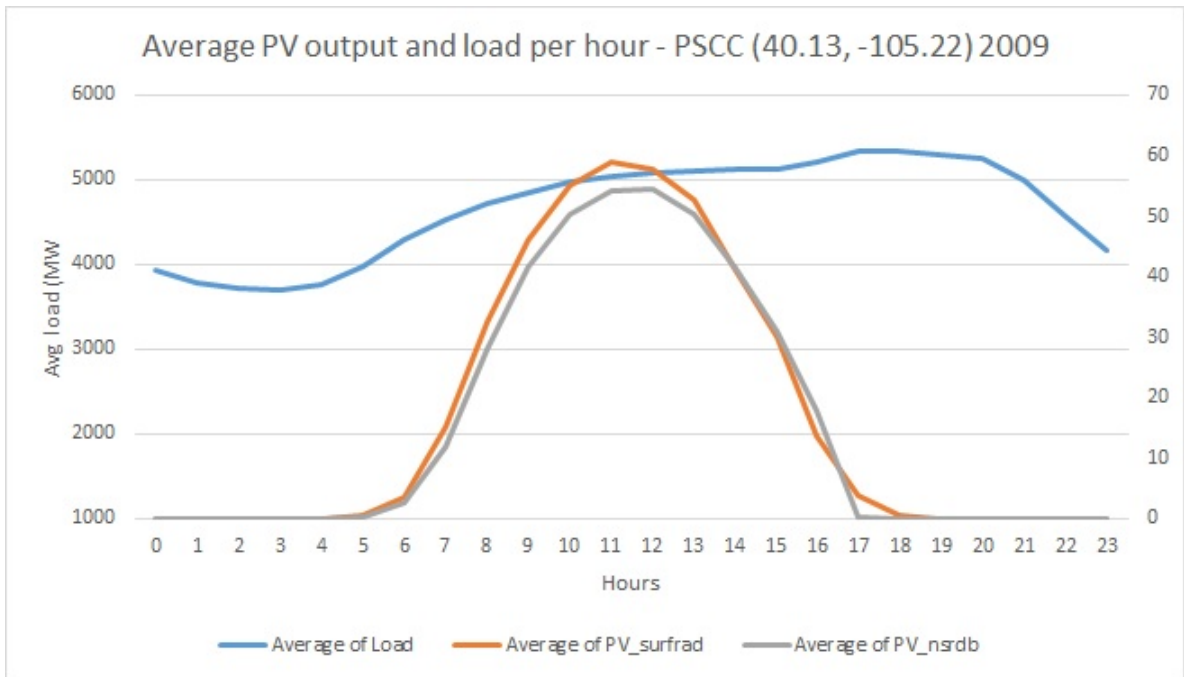


Figure 5.17: Colorado(2009) - Average load, average PV output from measured and modeled radiation data for hours of the day for all the days of the year.

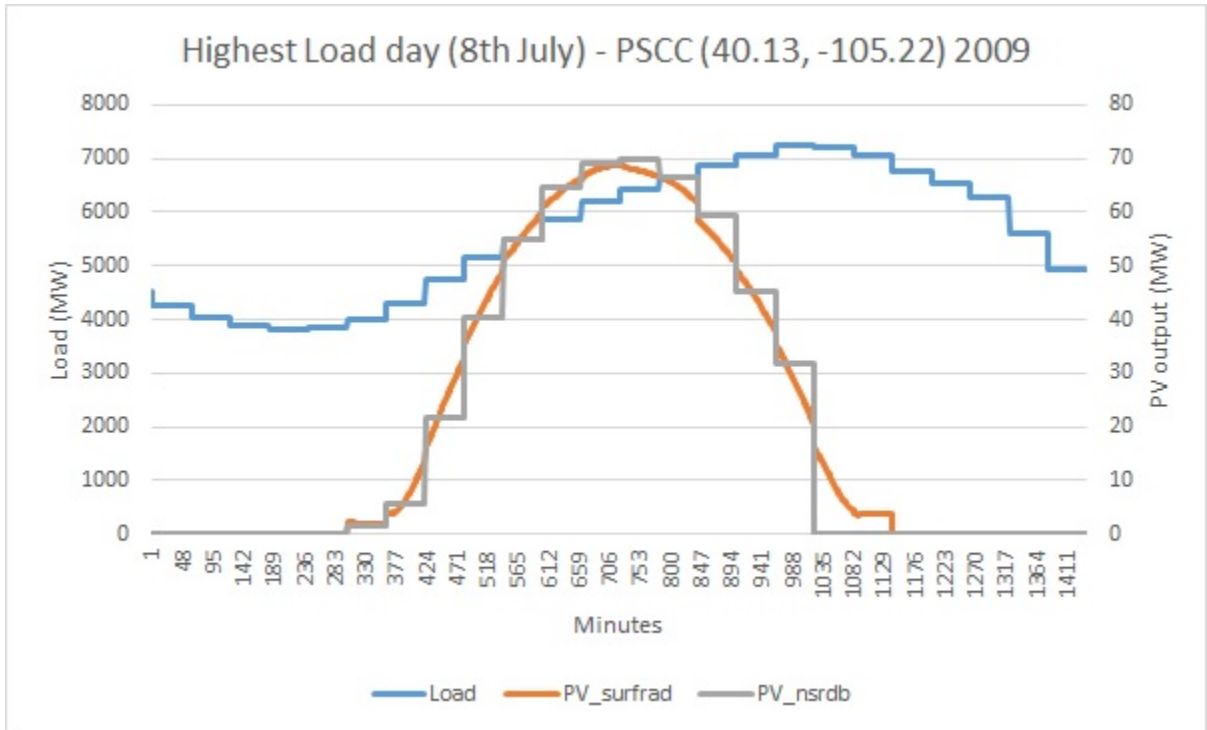


Figure 5.18: Colorado(2009) - Load and PV output on the highest load day.

Chapter 6: Conclusion and Future Work

The first part of this thesis reviews the current methodologies used for evaluating the capacity value of a solar power plant, and summarizes previous studies which use these capacity value techniques.

For our research, we study the effect of potential data issues on ELCC estimation. We find that hourly solar radiation data may not be as accurate as subhourly solar radiation data in estimating capacity value of a solar PV plant when we consider a single year under our study. Though, this error does smooth out when we use multiple years of data for our analysis. Errors in ELCC estimates derived from errors in recording or interpreting load data does not show a similar trend as in the case of ELCC estimates using hourly solar data. These errors do not smooth out by using multiple years of data. We also find that modeled solar radiation data introduce significant errors in capacity value estimates. We find that there are certain cases where data is missing for measured solar radiation data. This is another issue which has a drastic effect on the ELCC estimates. We have excluded these years from our analysis. Thus, our analysis shows that capacity value estimates for PV plants are highly sensitive to data issues.

For further study, it is possible to study the effect of such data issues on wind plants.

Bibliography

- [1] P. E. O. Aguirre, C. J. Dent, G. P. Harrison, and J. W. Bialek. Realistic calculation of wind generation capacity credits. In *Integration of Wide-Scale Renewable Resources Into the Power Delivery System, 2009 CIGRE/IEEE PES Joint Symposium*, pages 1–8, July 2009.
- [2] M. Amelin. Comparison of capacity credit calculation methods for conventional power plants and wind power. *IEEE Transactions on Power Systems*, 24(2):685–691, May 2009.
- [3] Hasan Fayazi Boroujeni, Meysam Eghtedari, Mostafa Abdollahi, and Elahe Behzadipour. Calculation of generation system reliability index: Loss of load probability. *Life Science Journal*, 9(4), 2012.
- [4] C. D’Annunzio and S. Santoso. Noniterative method to approximate the effective load carrying capability of a wind plant. *IEEE Transactions on Energy Conversion*, 23(2):544–550, June 2008.
- [5] K. Dragoon and V. Dvortsov. Z-method for power system resource adequacy applications. *IEEE Transactions on Power Systems*, 21(2):982–988, May 2006.
- [6] R. Duignan, C. J. Dent, A. Mills, N. Samaan, M. Milligan, A. Keane, and M. O’Malley. Capacity value of solar power. In *2012 IEEE Power and Energy Society General Meeting*, pages 1–6, July 2012.
- [7] L. L. Garver. Effective load carrying capability of generating units. *IEEE Transactions on Power Apparatus and Systems*, PAS-85(8):910–919, Aug 1966.
- [8] Thomas N Hansen. Utility solar generation valuation methods. *Department of Energy, Solar America Initiative Project*, 2008.
- [9] Thomas E Hoff, Richard Perez, Gerry Braun, Michael Kuhn, and Ben Norris. The value of distributed photovoltaics to austin energy and the city of austin. *Final Report to Austin Energy (SL04300013)*, 2006.

- [10] Y. Huang, C. Liu, G. He, X. Xu, J. He, W. Wang, and X. Zhou. Capacity value of pv generation and its impact on power system planning: A case study in north-west of china. In *2010 Asia-Pacific Power and Energy Engineering Conference*, pages 1–4, March 2010.
- [11] A. Keane, M. Milligan, C. J. Dent, B. Hasche, C. D’Annunzio, K. Dragoon, H. Holttinen, N. Samaan, L. Soder, and M. O’Malley. Capacity value of wind power. *IEEE Transactions on Power Systems*, 26(2):564–572, May 2011.
- [12] K. MacLaury. “assessing minnesotas solar resource - revenue implications of solar pv system orientation and rate structure”. The Minneapolis Saint Paul Solar Cities Program, 2011.
- [13] S. H. Madaeni, R. Sioshansi, and P. Denholm. Estimating the capacity value of concentrating solar power plants: A case study of the southwestern united states. *IEEE Transactions on Power Systems*, 27(2):1116–1124, May 2012.
- [14] S. H. Madaeni, R. Sioshansi, and P. Denholm. Comparing capacity value estimation techniques for photovoltaic solar power. *IEEE Journal of Photovoltaics*, 3(1):407–415, Jan 2013.
- [15] S. H. Madaeni, R. Sioshansi, and P. Denholm. Estimating the capacity value of concentrating solar power plants with thermal energy storage: A case study of the southwestern united states. *IEEE Transactions on Power Systems*, 28(2):1205–1215, May 2013.
- [16] Michael Milligan and Brian Parsons. A comparison and case study of capacity credit algorithms for wind power plants. *Wind Engineering*, 23(3):159–166, 1999.
- [17] Michael Milligan and Kevin Porter. The capacity value of wind in the united states: Methods and implementation. *The Electricity Journal*, 19(2):91–99, 2006.
- [18] Sophie Pelland and Ihab Abboud. Comparing photovoltaic capacity value metrics: A case study for the city of toronto. *Progress in Photovoltaics: Research and Applications*, 16(8):715–724, 2008.
- [19] Richard Perez. Photovoltaic capacity valuation methods. 2008.
- [20] Richard Perez and T Hoff. Energy and capacity valuation of photovoltaic power generation in new york. *Published by the New York Solar Energy Industry Association and the Solar Alliance*, 2008.
- [21] Richard Perez, R Margolis, M Kmiecik, M Schwab, and M Perez. Update: Effective load carrying capability of photovoltaics in the united states. In *Proc. ASES Annual Conference, Denver, CO*. Citeseer, 2006.

- [22] Thomas Rader. *Comparing Estimates of the Capacity Values of Photovoltaic Solar Power Plants Using Hourly and Sub-hourly Data*. PhD thesis, The Ohio State University, 2012.
- [23] L. Soder and M. Amelin. A review of different methodologies used for calculation of wind power capacity credit. In *Power and Energy Society General Meeting - Conversion and Delivery of Electrical Energy in the 21st Century, 2008 IEEE*, pages 1–5, July 2008.